ELSEVIER

0144-8617(95)00120-4

Carbohydrate Polymers 29 (1996) 169–181

0144-8617/96 $15.00+.00

A study of the rheological behavior of scleroglucan weak gel systems

Mario Grassi, Romano Lapasin & Sabrina Pricl*

Department of Chemical, Environmental and Raw Materials Engineering—DICAMP, University of Trieste, Piazzale Europa 1, I-34127 Trieste, Italy

(Received 2 June 1995; revised version received 14 August 1995; accepted 19 August 1995)

This study deals with the rheological behavior of aqueous systems of scleroglucan, the neutral polysaccharide secreted exocellularly by certain fungi of the genus *Sclerotium*. We investigated several aqueous systems under different temperatures and polymer concentrations by means of continuous and oscillatory flow procedures. Continuous shear flow tests revealed that a transition exists between a sol-like and a weak gel behavior for those scleroglucan systems in a polymer concentration range between 0.2 and 0.3% w/w. All systems exhibit marked non-Newtonian properties, which change from shear-thinning in the solution domain to plastic in the gel domain; however, the shear-dependent behavior of all systems can be satisfactorily described by a modified Cross equation. As far as the time-dependent properties are concerned, all scleroglucan aqueous systems exhibit a thixotropic response; stress transient experiments show that a delay time of approximately 4–5 min is necessary to remove shear history and to reconfigure the unperturbed state. Both classical dynamic measurements and parallel superposed continuous and oscillatory shear tests confirm the sol–gel transition for scleroglucan aqueous systems, and highlight the weak, transient nature of this microbial polysaccharide gel state. Copyright © 1996 Elsevier Science Ltd

INTRODUCTION

Scleroglucan is the term given to a class of fungal, neutral capsular polysaccharides secreted exocellularly by certain inperfect fungi, particularly of the genus *Sclerotium*. The primary structure of scleroglucan from *Sclerotium glucanicum* has been characterized as a linear chain of β-1,3-linked D-glucose units with single D-glucose side chains linked β-1,6 every third unit of the main chain. The average molecular weights of scleroglucans vary upon the microorganism stains; several have M_w in the range $1.3–3.2\times10^5$ and most in the range $3.2\times10^5–6\times10^6$ (Rodgers, 1973; Sandford, 1982).

The solid state conformation of scleroglucan is a rod-like triple helix (also called a 'triplex'), which consists of three individual strands composed of six residues in the backbone per turn. The three strands of the triplex are held together by interstrand hydrogen bonds and the 1,6-linked β-D-glucopyranosyl side groups protrude from the outside of the triple helix (Bluhm *et al.*, 1982). Interestingly, this exocellular homoglucan maintains in water its rod-like triple helical structure (Yanaki & Norisuye, 1983) whereas, when dissolved in dimethylsulfoxide (DMSO) or in sodium hydroxide (NaOH) $\geq$ 0.1 M, the helices dissociate and the individual chains assume a random coil configuration (Yanaki *et al.*, 1981).

Although scleroglucan has still to be approved for food and pharmaceutical use by the relevant organizations, it finds a number of potential uses as suspending, coating and gelling agents for the food and the cosmetic industry (Brigand, 1993); moreover, other fundamental characteristics shown by this biopolymer such as biocompatibility, biodegradability and bioadhesivity could be considered in the formulation of controlled release drug delivery systems (Grassi *et al.*, 1995). In fact, scleroglucan plays a major role in the petroleum industry, especially in enhanced oil recovery operations, by virtue of its high viscosity at low concentrations, and its good salt and temperature tolerance.

Despite the practical interest of this biopolymer, only a very few papers have appeared in the literature concerning a rheological characterization of scleroglucan aqueous systems (Biver *et al.*, 1986; Lapasin *et al.*, 1990). Therefore, the aim of this paper is to present a thorough investigation of the rheological properties of scleroglucan aqueous systems under different temperature and polymer concentration conditions, in order to

*Author to whom correspondence should be addressed.

clarify the process of sol–gel transition and to better characterize the gel phase from the standpoint of its mechanical properties.

MATERIALS AND METHODS

Preparation of scleroglucan systems

The scleroglucan sample (zero-shear rate intrinsic viscosity at 25°C $[\eta]_0 = 21.53$ dl g^{-1}) was kindly supplied by VectorPharma Intl. S.p.A. (Trieste, Italy). All aqueous systems were prepared by swelling a proper amount of freeze-dried polymer with drops of twice-distilled water. The viscous material so formed was adjusted in concentration by the addition of water or NaOH 0.1 M, under gentle stirring, and left to rest overnight. The final concentration C_p (% w/w) was determined by weighing both the lyophilized polymer (taking into account the water present in the solid) and the final solution.

The effect of polymer concentration on the rheological behavior of scleroglucan in water was studied at 25°C by considering the following C_p values: 0.13, 0.25, 0.38, 0.50, 0.62, 0.75, 1.00, 1.13 and 2.00, whereas the systems in NaOH were characterized by C_p values of 0.50, 0.75 and 1.00, respectively. Measurements were carried out at 15, 25, 35 and 45°C on those systems with $C_p = 0.38$, 0.62 and 1.13 in order to evaluate the temperature effects on the rheological properties of scleroglucan–water systems.

Apparatus and procedures

All rheological measurements were performed with two rotational rheometers, the Haake RV100 and the Haake RV20, both coupled with the measuring device CV100, mounted with a coaxial cylinder sensor system ZB15 (Couette type). The inner cylinder used with this coaxial sensor system has the following dimensions: 13.91 mm diameter, 32.30 mm length; the gap was 0.545 mm. During the tests, while the outer cup is driven, the inner cylinder is mechanically positioned and centered by an air bearing. The top and bottom surfaces of the inner cylinder are especially designed to minimize end effects.

Additional sets of experimental data were obtained, in oscillatory shear flow regime, for scleroglucan aqueous systems with $C_p = 0.20$, 1.00 and 2.00, with a sensitive prototype cone-and-plate rheometer for low deformation measurements, designed and constructed by Dr Robert K. Richardson of the Department of Food Research and Technology, Silsoe College, Bedford, UK.

Stepwise procedures were applied for the analysis of the shear- and time-dependent properties in continuous shear flow conditions.

The multiple-step procedure consisted of a sequence of different shear rates $\dot{\gamma}$, each shear rate being kept constant until a steady value of the shear stress τ_s was attained. The analysis of the shear-dependent properties could then be properly based upon the steady values of the shear stress obtained at the different shear rates, whereas the sequence of stress transients allowed an inspection of the nature and the extent of the time-dependent properties to be performed.

It is important to emphasize here that the relationship between the shear rate $\dot{\gamma}$ and the shear stress τ (that is, the shear viscosity) can be obtained from the raw experimental data only in the case of Newtonian fluids. Indeed, for non-Newtonian systems it is necessary to consider the existence of a shear rate distribution in the gap and hence to calculate the 'effective shear rate' at the inner cylinder wall. Starting with the integral equation which relates the angular velocity Ω to the effective shear rate:

$$\Omega = \int_{\tau_o}^{\tau_i} \dot{\gamma}(\tau)/2\tau \, d\tau \tag{1}$$

where τ_i and τ_o are the tangential stresses at the inner and outer cylinder walls, respectively, and $\dot{\gamma}(\tau)$ is the unknown quantity, a number of approximate methods have been proposed in the literature for calculating shear rates in coaxial cylinder viscometers. In this paper, we use the method suggested by Yang and Krieger (1978), which is based on the derivation of both members of equation (1) and on an expression of $\dot{\gamma}(\tau)$ as a truncation of a convergent infinite series. In particular, the effective shear rates $\dot{\gamma}$ have been calculated according to the truncated form given by equation (7) in the Yang and Krieger paper, and the corresponding values have been reported throughout this work.

Flow curves (shear stress vs effective shear rate plots) were fitted by using computerized non-linear regression analysis.

The analysis of time-dependent properties (shear stress growth after initiation of a constant shear rate as a function of time) was performed according to the single step or on–off procedure suggested by Trapeznikov and Fedotova (1954). Here, a shear rate is applied and kept constant until a steady value of the stress is attained and, then, it is suddenly removed. After a given rest time t_r, the same stepwise variation of the shear rate is carried out. If this procedure is repeated for different rest times and, accordingly, different stress transients are recorded, information can be obtained on the time-dependent properties of the systems and on their dependence on different rest times. It is necessary to remark here that all data obtained from transient experiments are affected, more or less seriously, by instrumental effects such as finite time for start-up or stop, motor control with possible motor overshooting, inertia of the system and data filtering. Nevertheless, all results can still be used on a comparative basis.

Dynamic measurements were carried out to investigate the viscoelastic properties of these materials at 25°C. During the tests in oscillatory flow conditions, the shear strain imposed on the material is described by the expression:

$$\gamma = \gamma^0 \sin(\omega t) \tag{2}$$

where t is the time, ω is the frequency of oscillation and γ^0 is the maximum shear strain. In the linear viscoelastic regime, a sinusoidal stress response of the same frequency, having amplitude τ^0 and phase lag δ, is obtained, so that the dynamic moduli G' and G'' can be derived straight from the experimental data. When the applied strain exceeds a critical value γ^0_c, the viscoelastic behavior becomes non-linear, and the resultant periodic shear stress can be properly expressed by the Fourier series:

$$\tau = \gamma^0 \sum_{k,odd} [G'_k \sin(kt) + G''_k \cos(kt)] \tag{3}$$

in which each of the k harmonics is characterized by the coefficients G'_1 and G''_1. With increasing strain, the weight of higher order harmonics, and specifically of the third harmonic, may become substantial; nevertheless, if the ratio of the amplitude of the third and fifth harmonic does not exceed 5%, the in-phase and the out-of-phase components of the fundamental harmonic, G'_1 and G''_1, can still be used to characterize, albeit with a certain degree of approximation, the elastic and viscous contribution to the entire response of the material (Lapasin & Pricl, 1995).

Calibration of the apparatus was performed by carrying out measurements on Newtonian fluids, in order to evaluate both the response linearity of these systems under the selected operative conditions and to develop a standard procedure for the correction of the inertial effects. The strain dependence of the viscoelastic quantities for scleroglucan aqueous systems with $C_p = 0.20$, 1.00 and 2.00 was investigated with the prototype rheometer through strain sweeps in the range 10^{-4}–10^{-1} at a fixed frequency of oscillation $\omega = 10$ rad/s. Frequency sweeps in the range 10^{-1}–10^{2} rad/s were performed on the same samples at a constant strain value $\gamma^0 = 2 \times 10^{-2}$.

An analysis of the transition from linear to non-linear viscoelastic regime was performed by carrying out strain sweeps (from 5×10^{-2} to 2.5) at four different frequencies (0.63, 1.26, 3.14 and 12.6 rad/s) on the samples with $C_p = 0.20$ and 1.00 by using the Haake RV20-CV100 configuration.

Tests under parallel superposition of steady and oscillatory flow conditions were performed with the Haake RV100-CV100 at a constant strain of 2.4 in a frequency range 0.314–6.28 rad/s and in a shear rate range for 0.3 up to 3 s^{-1} on scleroglucan aqueous systems with $C_p = 0.25$ and 1.00.

RESULTS AND DISCUSSION

Continuous shear flow tests

Shear-dependent properties

The tests carried out under continuous shear conditions revealed that all the scleroglucan aqueous systems examined exhibited marked non-Newtonian properties; moreover, all those samples having a C_p greater than 0.25 showed the same rheological behavior, characterized by a slight increase in the shear stress value τ determined at the same shear rate $\dot{\gamma}$ with increasing C_p.

With the aim of performing a correct analysis of experimental data, the effective values of the applied shear rate were calculated by using the Yang and Krieger method (see the Materials and Methods). The results obtained from the application of this procedure showed that the effective $\dot{\gamma}$ values differed from the nominal ones to an extent that, in some cases reached 100%. As an example, we report in Fig. 1 the relative differences between the corresponding effective and nominal shear rate $\Delta(= (\dot{\gamma} - \dot{\gamma}_{nom})/\dot{\gamma}_{nom})$ for the most dilute and concentrated systems, respectively. As expected, the most pronounced differences were found in the middle shear rate region, where the strongest deviations from Newtonian behavior occurred.

Figure 2 is a plot of the data for the shear stress τ as a function of the effective shear rate $\dot{\gamma}$ for a set of systems considered in this work. The flow curves in Fig. 2 show that, except for those samples with $C_p \leqslant 0.25$, the evidence of a yield stress becomes apparent. As a consequence, the description of such a rheological behavior could be properly achieved by means of a pseudoplastic model for the low concentration samples and by a model of the plastic type for all other systems. Nevertheless, it would be more convenient to resort to a unique rheological equation for the data fitting, in order

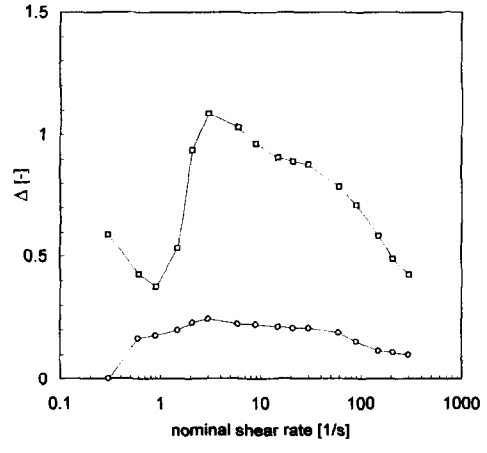

Fig. 1. Relative differences Δ between the corresponding effective and nominal shear rate vs nominal shear rates for two scleroglucan systems: (○), $C_p = 0.13$; (□), $C_p = 2.00$. $T = 25$°C.

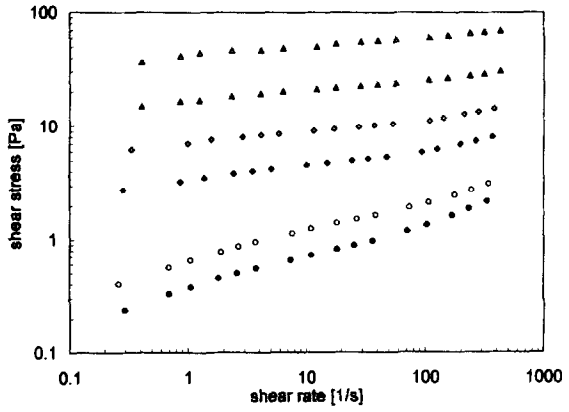

Fig. 2. Flow curves for scleroglucan aqueous systems at different polymer concentrations: (●), $C_p=0.13$; (○), $C_p=0.25$; (◆), $C_p=0.38$; (◇), $C_p=0.75$; (▲), $C_p=1.13$; (△), $C_p=2.00$. $T=25°C$.

both to describe the effects of polymer concentration on the rheological properties of these polysaccharide aqueous systems and to determine a boundary concentration value C_0, corresponding to the transition between a pseudoplastic and a plastic behavior.

Several simple models have been proposed and used in literature to describe the viscosity of many polymeric fluids that exhibit Newtonian behavior at low shear rates and power law behavior at high rates of deformation, such as the Cross and the Carreau equations (Cross, 1965; Carreau, 1968). On the other hand, for the prediction of the viscosity at a given shear rate of those systems which exhibit a yield stress and a shear thinning behavior at high rates of deformation, Poslinski *et al.* (1988) proposed a modified Carreau equation, containing a yield term τ_y, which has been successfully applied to other polysaccharide systems (Delben *et al.*, 1990). For a comprehensive description of the rheological behavior of the systems under investigation, we suggest a modification of the complete form of the Cross equation, as reported below:

$$\tau = \tau_y + \eta_\infty\dot{\gamma} + \frac{(\eta_0 - \eta_\infty)\dot{\gamma}}{1 + (\lambda\dot{\gamma})^n} \tag{4}$$

where τ_y is the yield stress, η_0 is the zero-shear rate viscosity (lower Newtonian plateau), η_∞ is the infinite-shear rate viscosity (upper Newtonian plateau), λ is a characteristic time and n is a dimensionless exponent. It should be noted here that, in the case of plastic systems, the zero-shear viscosity η_0 represents the estimated value for the viscosity the system would have if it maintained a typical solution behavior for low values of $\dot{\gamma}$. Table 1 reports the values of the parameters of the modified Cross model for all scleroglucan aqueous systems at 25°C. As can be observed from Table 1, the only remarkable variations in the parameter values are those relative to the yield stress τ_y and the zero-shear rate viscosity η_0.

A further glance at Table 1 reveals also that, only for those systems having $C_p \geqslant 0.38$, data fitting provides an appreciable value of the yield stress τ_y. The onset of a plastic behavior is generally ascribed to the existence of a three-dimensional network under limiting shear conditions (i.e. $\dot{\gamma}\to 0$). For such systems as those studied here, we can consider that the meaningful values of τ_y can be taken as an indication of the presence of a three-dimensional supermolecular structure typical of a physical gel state. In this sense, we can assume for $\tau_y(C_p)$ the same functional dependence derived from the percolation theory for the elastic modulus of gels (de Gennes, 1979):

$$\tau_y = K(C_p - C_0)^m \tag{5}$$

where C_0 is the threshold concentration for the sol–gel transition. In our case, a good correlation of data was obtained for $K=12.2$ Pa, $C_0=0.23$ and $m=1.01$ (see

Table 1. Values of the parameters of the modified Cross model for all scleroglucan systems at 25°C

C_p (% w/w)	τ_y (Pa)	η_0 (Pa.s)	$\eta_\infty \times 10^3$ (Pa.s)	λ (s)	n (—)	ARD[a] ×100
0.13	0.08	1.05	2.5	3.39	0.797	0.30
0.25	0.22	1.03	2.4	1.61	0.814	0.36
0.38	2.21	2.85	5.7	1.58	0.885	0.36
0.50	3.43	4.03	2.9	1.34	0.869	0.33
0.63	4.63	5.28	8.0	2.20	0.874	0.56
0.75	5.20	4.50	8.7	1.47	0.898	0.38
1.00	7.92	9.63	10.4	2.07	0.900	0.59
1.13	11.9	13.9	8.6	2.17	0.878	0.38
2.00	29.0	45.4	11.7	3.01	0.878	0.90

C_p, final concentration; τ_y, yield stress; η_0, zero-shear rate viscosity; η_∞, infinite shear rate viscosity; λ, characteristic time; n, dimensionless exponent.

[a]Average relative deviation $= \dfrac{\sum_{i=1}^{N}\left|\dfrac{\tau_i^{exp} - \tau_i^{calc}}{\tau_i^{exp}}\right|}{N}$

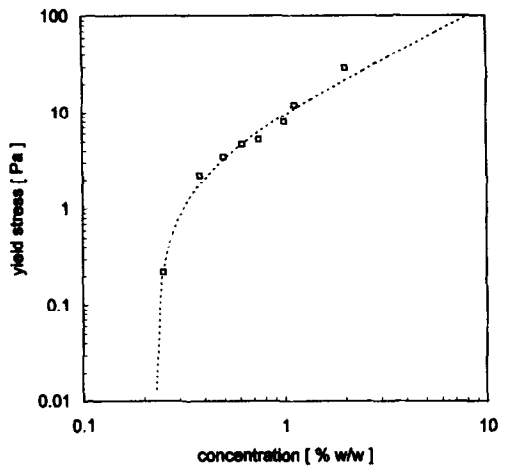

Fig. 3. Yield stress τ_y vs scleroglucan concentration C_p: (□) τ_y values estimated from experimental data with equation (4); (– – –) correlation with equation (5).

Fig.). This concentration dependence was slightly weaker than that observed for other polysaccharide physical gels (Lapasin & Pricl, 1995) and much weaker than that usually detected for a number of other viscoplastic materials (Bird *et al.*, 1983).

The shear-dependent behavior just described is typical of weak gel systems, for which the application of large or continuously increasing deformations leads to the progressive breakdown of their networks into smaller clusters. Accordingly, the systems can flow homogeneously, with flow properties typical of disperse systems. This is not the case for strong gels which, when subjected to large deformations or continuous flow conditions, undergo network ruptures with discontinuity surfaces running throughout the system. Necessarily, then, the flow conditions become heterogeneous.

The tests carried out on the scleroglucan samples with $C_p = 0.38$, 0.62 and 1.13 showed that the temperature has only a slight effect on the shear-dependent properties of these systems. In detail, the parameter which controls the low shear behavior of these materials, the yield stress τ_y, does not practically vary with increasing temperature from 15 to 45°C, as evidenced by the relevant values reported in Table 2. Such evidence can be considered as the consequence of the increasing contribution of the polymeric disperse phase to the system viscosity as the temperature increases. This fact can be easily highlighted by reconsidering the experimental data in terms of relative viscosity η_r, defined as the ratio of system viscosity and water viscosity. Figure 4 shows the relative viscosity of the system with $C_p = 0.38$, calculated at five shear rate values with equation (4) and expressed in a normalized form, taking the value of the relative viscosity at 15°C as a reference. As we can see, the relative viscosity increases with increasing temperature. This could be ascribed to the favorable effect exerted

Table 2. Parameters of the modified Cross model at different temperatures for three scleroglucan systems

C_p (% w/w)	T (°C)	τ_y (Pa)	η_0 (Pa.s)	$\eta_\infty \times 10^3$ (Pa.s)	λ (s)	n (—)
0.38	15	2.17	5.50	6.55	2.91	0.88
	25	2.21	2.85	5.70	1.58	0.88
	35	2.35	3.09	4.50	1.65	0.87
	45	2.43	2.10	3.85	0.95	0.89
0.62	15	4.40	6.27	8.50	3.17	0.85
	25	4.63	5.28	8.00	2.20	0.87
	35	4.63	4.50	6.50	1.66	0.88
	45	4.44	3.54	5.76	1.21	0.89
1.13	15	14.1	6.49	2.50	1.47	0.82
	25	11.9	13.9	8.60	2.17	0.88
	35	15.1	2.85	4.10	0.56	0.84
	45	6.37	8.68	1.00	0.62	0.89

T, temperature. For other abbreviations see Table 1 footnote.

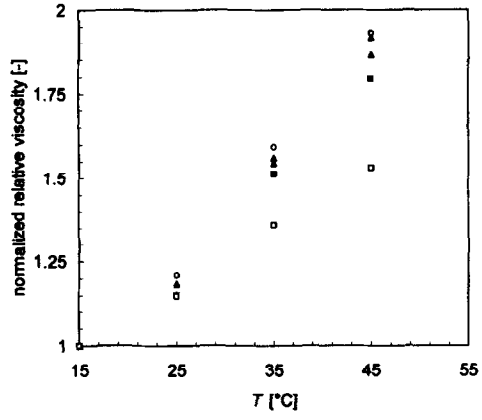

Fig. 4. Normalized relative viscosity ($\eta_r(T)/\eta_r(15°C)$) vs temperature T for the scleroglucan system with $C_p = 0.38$, calculated with equation (4) at five different shear rates: (○), $\dot{\gamma} = 0.1\ s^{-1}$; (▲), $\dot{\gamma} = 1\ s^{-1}$; (△), $\dot{\gamma} = 10\ s^{-1}$; (■), $\dot{\gamma} = 100\ s^{-1}$; (□), $\dot{\gamma} = 1000\ s^{-1}$.

by the temperature on the degree of intermolecular association, which results in the presence, even under medium–high shear rate conditions, of aggregates whose dimensions increase with increasing temperature. An alternative, sensible explanation could be found by considering a change in the degree of swelling of the macromolecular aggregates, leading to a greater effective volume of the disperse phase.

Further proof of the role played by the rigid rod-like conformation of scleroglucan triple helix in the formation of supermolecular structures in water can be obtained by considering the rheological behavior of this biopolymer system in 0.1 M NaOH. In fact, besides the absolute values of the shear viscosity which, for a given scleroglucan system in NaOH, is of orders of magnitude lower than the corresponding value in water, in its random coil configuration, this polysaccharide shows a very weak non-Newtonian character, as depicted in Fig. 5. This flow behavior is expected for single flexible random coils, which show

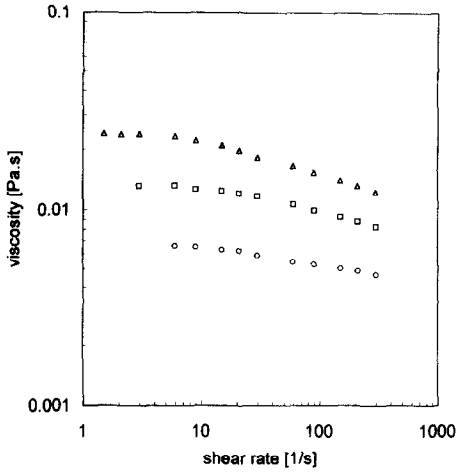

Fig. 5. Steady shear viscosity η vs shear rate $\dot{\gamma}$ for three scleroglucan systems in 0.1 M NaOH: (○), $C_p = 0.50$; (□), $C_p = 0.75$; (Δ), $C_p = 1.00$. $T = 25°C$.

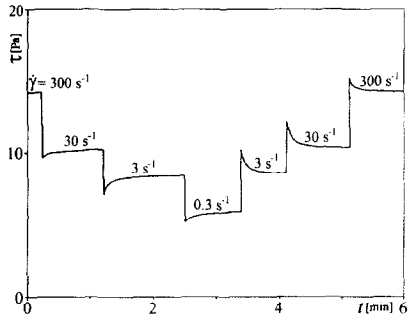

Fig. 6. Shear stress transients in step-shear rate tests for the scleroglucan system with $C_p = 0.75$. $T = 25°C$.

far less anisotropy and shear orientation than the rigid helices and which give rise to an entanglement network in solution.

Time-dependent properties

All scleroglucan systems belonging to the weak gel domain show appreciable time-dependent properties of the thixotropic type. As shown in Fig. 6, relative to the system with $C_p = 0.75$, stress transients, corresponding to structural breakdown and build-up processes, regularly result from sudden, stepwise $\dot{\gamma}$ variations of opposite sign. The amplitude and the kinetics of these structural processes depend on the amplitude of the shear rate variation and on the instantaneous shear rate value, respectively; such effects, however, are more pronounced at lower values of the shear rate. For these scleroglucan systems, the effects the structural processes have on their time-dependent behavior are strong enough to conceal the viscoelastic features of the stress response, related to the intrinsic deformability and elasticity of the biopolymer aggregates. As can be seen in Fig. 6, the steady stress values attained at each constant shear rate are independent of the previous rheological history so indicating that the time-dependent properties of these materials are reversible; furthermore, an undershoot in the stress is observed when $\dot{\gamma}$ is decreased and a stress overshoot is observed when $\dot{\gamma}$ is increased (see Fig. 6), which is equivalent to saying that scleroglucan weak gels behave as canonical thixotropic systems.

The reason for such typical thixotropic behavior can be easily explained by considering that the stress values in structured biopolymer systems are determined by the existence of large scale structures; these, in turn, are characterized by the shear history experienced by the systems themselves. At higher rates of deformation, the eventually surviving structures are smaller in size; as a consequence, when $\dot{\gamma}$ is suddenly decreased, τ first undershoots its equilibrium value and then slowly increases as the structures redevelop to larger, equilibrium dimensions characteristic of the new applied rate of shear. Analogous arguments can be used to explain the presence of stress overshoots.

The stress transient obtained at constant $\dot{\gamma}$ can be suitably described by the following stretched exponential function:

$$\tau = \tau_s + (\tau_i - \tau_s)\exp[(-t/t_c)^n] \tag{6}$$

in which τ_i and τ_s represent the initial and stationary values of the stress, respectively, t_c is a characteristic time for the exponential decay and n is a numerical exponent which modulates the transient behavior of the stress. Almost analogous results can be obtained by using the following relationship:

$$\tau = \frac{1}{\left[\frac{1}{\sqrt{\tau_s}} + \left(\frac{1}{\sqrt{\tau_i}} - \frac{1}{\sqrt{\tau_s}}\right)\exp(-kt)\right]^2} \tag{7}$$

where τ_i and τ_s have the same meaning as in equation (6) and k is a kinetic constant.

In the present analysis of scleroglucan stress transients we preferred to use equation (7) mainly for two reasons. Firstly, equation (7) contains only three adjustable parameters whereas equation (6) is a four-parameter model; moreover, equation (7) derives from a more general approach to the description and interpretation of thixotropy (see Appendix A).

Table 3 reports, as an example, the results obtained for the system with $C_p = 0.75$, whose time-dependent behavior has been illustrated in Fig. 6. As we can see, the extent of the time-dependent phenomenon, expressed by the ratio $\Delta\tau/\tau_s$, is more pronounced in the middle–low shear rate range. The kinetics of the $\tau(t)$ variations is faster at higher $\dot{\gamma}$; moreover, a comparison of the values of the kinetic constant k reveals that the kinetics of the structural breakdown processes is faster than that of the corresponding build-up.

Undoubtedly more complex is the analysis of the data obtained from the application of the on–off procedure. Here, the purpose of the experimental investigation is the evaluation of the amplitude and the kinetics of the

Table 3. Values of τ_i, τ_s, k and $\Delta\tau/\tau_s$ calculated using equation (7) for the scleroglucan system with $C_p = 0.75$ at 25°C

From $\dot{\gamma}$ (s^{-1})	To $\dot{\gamma}$ (s^{-1})	τ_i (Pa)	τ_s (Pa)	k (s^{-1})	$\Delta\tau/\tau_s$ (—)
30	300	15.15	14.33	0.44	0.057
300	30	9.72	10.33	0.15	0.059
3	30	12.19	10.33	0.27	0.180
30	3	7.22	8.45	0.19	0.145
0.3	3	10.21	8.45	0.23	0.209
3	0.3	5.15	5.81	0.14	0.113

$\dot{\gamma}$, shear rate; τ_i, initial stress; τ_s, stationary stress; k, kinetic constant; $\Delta\tau/\tau_s$, extent of time-dependent phenomenon.

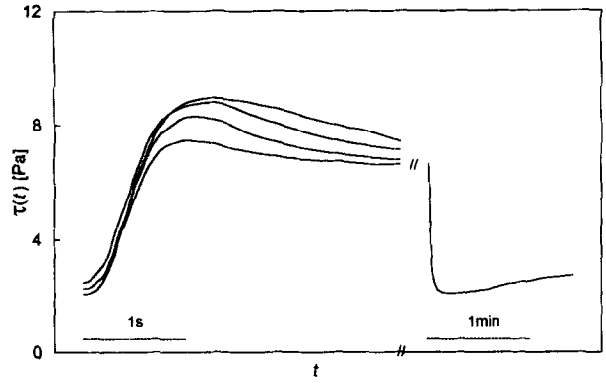

Fig. 7. (a) Stress growth upon inception of shear flow ($\dot{\gamma} = 3\ s^{-1}$) after four different rest times (from bottom to top: $t_r = 5''$; $t_r = 15''$; $t_r = 30''$; $t_r = 1'$); and (b) stress relaxation after steady shear flow ($\dot{\gamma} = 3\ s^{-1}$). $C_p = 0.62$; $T = 25$°C.

build-up process under rest conditions. Figure 7 reports the results obtained at $\dot{\gamma} = 3\ s^{-1}$ and after four different rest times for the scleroglucan systems with $C_p = 0.62$. As the rest time t_r increases, the stress overshoot increases and the characteristic time of the stress peak gradually shifts towards higher values, with a progressive modification of the shape of the corresponding $\tau(t)$ curve. Tests after the cessation of steady shear flow seem to confirm the plastic nature of the rheological behavior of these biopolymer systems (i.e. for those systems with $C_p \geq 0.2$–0.3), since the stress does not relax to zero but tends to a residual value τ_r (see Fig. 7) which, for each polymer concentration, is almost independent of the shear rate applied during the test. The numerical values of the residual stress τ_r are comparable to those of the apparent yield stress τ_y obtained from the fitting of the corresponding τ–$\dot{\gamma}$ data sets with equation (4).

The recovery properties of the materials under examination can be further exemplified by considering Fig. 8, in which the stress overshoot ratio τ^*, defined as the ratio of the peak shear stress maximum and the stress equilibrium value at the corresponding shear rate is reported as a function of the rest time t_r for four different scleroglucan concentrations at constant $\dot{\gamma} = 3\ s^{-1}$. As we can see, the structure rehealing process under rest

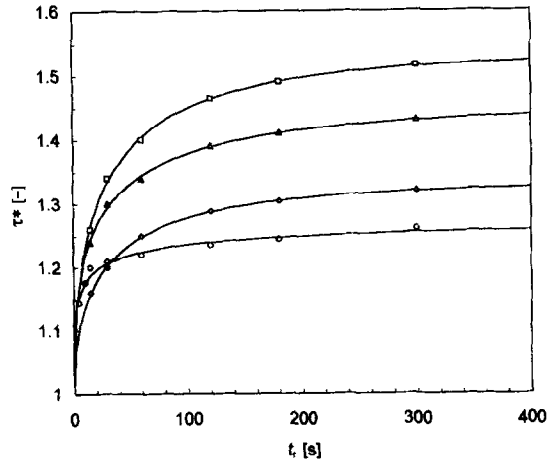

Fig. 8. Stress overshoot ratio τ^* as a function of the rest time t_r for four different scleroglucan systems at constant $\dot{\gamma} = 3\ s^{-1}$: (○), $C_p = 0.25$; (△), $C_p = 0.50$; (□), $C_p = 0.75$; (◇), $C_p = 1.00$; (———), experimental data correlation with equation (8). $T = 25$°C.

conditions develops to a considerable extent also for the system with $C_p = 0.25$ and becomes maximum for the systems with $C_p = 0.75$. The kinetics of the structural build-up process is characterized by a critical time, which increases with increasing polymer concentration. Both these aspects are reflected in the values of the two parameters τ^*_∞ and $t_{r,c}$, obtained by the fitting of the relevant $\tau^*(t_r)$ data with the following stretched exponential model:

$$\tau^* = \tau^*_\infty - (\tau^*_\infty - 1)\exp-(t_r/t_{r,c})^n \quad (8)$$

where t_r is the rest time interval, τ^*_∞ is the asymptotic value of the stress overshoot ratio for $t_r \to \infty$, $t_{r,c}$ is the critical rest time and n is a parameter characterizing the buildup kinetics. Table 4 reports the calculated values of τ^*_∞ and $t_{r,c}$ for the four systems considered in Fig. 8. From an inspection of Table 4 we can argue that a delay time of approximately 4–5 min is necessary to substantially (95%) remove shear history and to reconfigure the unperturbed state. Such a timescale for the recovery of non-linear properties is typical of weak gels characterized by a low connectivity such as xanthan (Richardson & Ross-Murphy, 1987) and *N*-(carboxymethyl) chitosan systems (Delben *et al.*, 1990).

Table 4. Values of τ^*_∞, $t_{r,c}$ and n calculated with equation (8) for four scleroglucan systems at 25°C

C_p (% w/w)	τ^*_∞ (Pa)	$t_{r,c}$ (s)	n (—)
0.25	1.26	8.5	0.33
0.50	1.45	27	0.45
0.75	1.53	31	0.53
1.00	1.33	33	0.54

C_p, final concentration; τ^*_∞, asymptotic value of the stress overshoot ratio for $t_r \to \infty$; $t_{r,c}$, critical rest time; n, parameter characterizing build-up kinetics.

Oscillatory shear flow tests

Linear viscoelastic properties

A preliminary step in the analysis of any oscillatory flow data should consist of checking the independence of instrumental responses of oscillation amplitude, i.e. the limit of the linear viscoelastic regime. As the strain γ^0 increases, the system response remains unchanged in terms of amplitude, expressed through the complex modulus G^*, and of the phase lag δ. At a certain point, a critical strain value γ^0_c is attained, above which we observe a progressive reduction of G^*, whereas δ begins to increase. γ^0_c then marks the limit of the viscoelastic regime within which it is possible to express, with a correct formalism, the entire material response in terms of G^* and δ or, alternatively, of the elastic and viscous components of G^*, the storage modulus G' and the loss modulus G'', respectively.

Figure 9a and b shows the results obtained from a strain sweep performed at constant frequency of oscillation $\omega = 3.14$ rad/s in a deformation range from 5×10^{-2} to 2.5 on scleroglucan systems with $C_p = 0.2$, 1 and 2. From an inspection of both response amplitude and phase lag, reported in a normalized form with the corresponding linear viscoelastic values as reference, we can determine the corresponding values of the critical strain γ^0_c, which fall in the strain range 0.15–0.20 for the 0.2 and 1% systems, and around 0.30 for the system with $C_p = 2$. Further strain sweeps performed with the prototype rheometer on scleroglucan systems with $C_p = 0.2$, 1 and 2 in a deformation range from 10^{-4} to 10^{-1} at constant $\omega = 10$ rad/s did not reveal any appreciable variation of the viscoelastic quantities.

As regards the dependence of the viscoelastic quantities G' and G'' on the imposed frequency of oscillation, Fig. 10a reports the mechanical spectra for three scleroglucan systems obtained at constant $\gamma^0 = 2\times10^{-2}$. For the system with $C_p = 0.2$, the corresponding $G'(\omega)$ and $G''(\omega)$ traces indicate that the rheological response of this system is shifted toward that exhibited by concentrated solutions, and does not share common features with those relative to the gel-like samples with $C_p = 1$ and 2. The transition from sol-like to gel-like behavior with increasing concentration of this microbial polysaccharide is even more noticeable when we consider the value of the phase lag δ reported in Fig. 10b. As C_p decreases, the viscous and elastic components come closer to one another; so, δ increases and tan δ shows a pronounced minimum. Minima in tan δ are typical of entanglement networks and correspond to a period of oscillation which is long compared to the relaxation times of entanglement network strands but short compared to the lifetime of those entanglements. Nevertheless, this and other evidence from amylose (Doublier & Choplin, 1989) and gelatin (Carnali, 1992) indicate that the minimum may occur also in various weak and strong gels; furthermore, these minima are

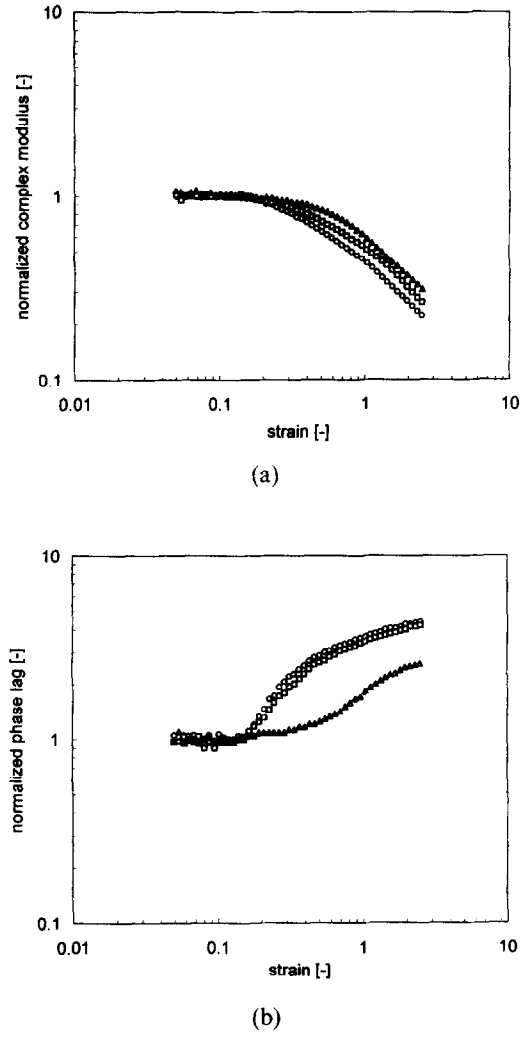

Fig. 9. (a) Normalized complex modulus and (b) normalized phase lag as a function of strain γ^0 at constant frequency of oscillation $\omega = 3.14$ rad/s for three scleroglucan systems: (Δ), $C_p = 0.20$; (□), $C_p = 1.00$; (○), $C_p = 2.00$. $T = 25$°C.

related to the sol fraction of the system and can be interpreted as signaling a truncation of the usual relaxation modes in the gel by a mechanism with a finite relaxation time.

The oscillatory linear viscoelastic data described above can be correlated with the generalized Maxwell model, which is derived from the parallel combination of N Maxwell elements. Each Maxwell element is characterized by a relaxation time λ_k, defined as the ratio of the dashpot Newtonian viscosity μ_k and the Hookean spring rigidity G_k. The constitutive equation for the corresponding generalized Maxwell fluid is obtained by summing the contribution τ_k of each of the N Maxwell elements:

$$\tau = \sum_{k=1}^{N} \tau_k \tag{9}$$

where each contribution τ_k is given by the constitutive equation of the Maxwell element:

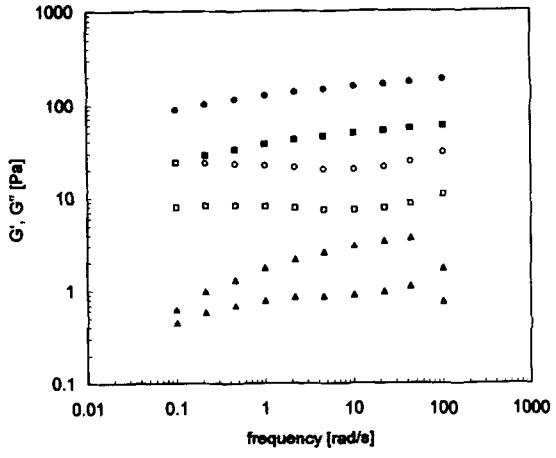

(a)

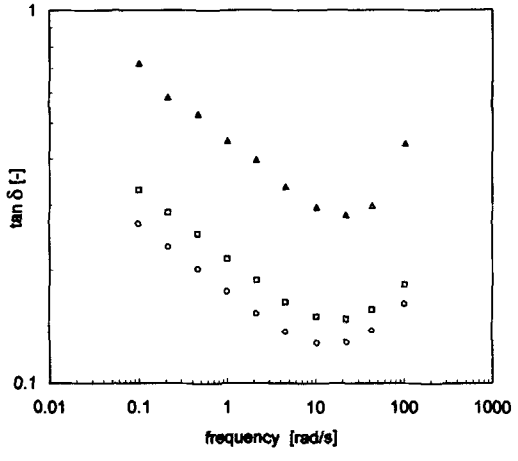

(b)

Fig. 10. (a) Dynamic moduli and (b) loss tangent vs imposed oscillation frequency ω at constant strain $\gamma^0 = 0.02$ for three scleroglucan systems. (a) (▲), G', (Δ), G'': $C_p = 0.20$; (■), G', (□), G'': $C_p = 1.00$; (●), G', (○), G'': $C_p = 2.00$. (b) (Δ), $C_p = 0.20$; (□), $C_p = 1.00$; (□), $C_p = 2.00$. $T = 25°C$.

$$\tau_k + \lambda_k \frac{\partial \tau_k}{\partial t} = G_k \dot{\gamma} \tag{10}$$

Accordingly, the model yields the following expressions for the viscoelastic quantities under small-amplitude oscillatory motion:

$$G' = \sum_{k=1}^{N} \frac{G_k \lambda_k^2 \omega^2}{1 + (\lambda_k \omega)^2} \tag{11}$$

$$G'' = \sum_{k=1}^{N} \frac{G_k \lambda_k \omega}{1 + (\lambda_k \omega)^2} \tag{12}$$

We have chosen to fit the G' and G'' data reported in Fig. 10 to eight relaxation times, logarithmically spaced between approximately 10^{-3} and 10^3 s. Under this condition, the non-linear regression of the experimental data yielded the best set of G_k, together with λ_1 and the scale factor λ_{k+1}/λ_k. The results of this numerical procedure can be conveniently expressed through the corresponding relaxation time distribution $G_k(\lambda_k)$, as reported in Fig. 11. As we can see from this figure, the relaxation spectra for the scleroglucan systems with $C_p = 1.00$ and 2.00 are extended to large relaxation times and have a box-type shape, typical of structured systems. The third distribution in Fig. 11, relative to the system with $C_p = 0.20$, decays to negligible values for relaxation times of about 50 s; such behavior can be, at least to a rough approximation, considered close to that of a concentrated polymeric solution.

At the end of this section, it is worthwhile considering the comparison between the experimental data obtained under continuous and oscillatory flow conditions. In fact, the verification of the validity or, alternatively, the failure of the empirical Cox–Merz rule (Cox & Merz, 1958), which states that the magnitude of the complex viscosity $\eta^*(\omega)$ and the steady shear viscosity $\eta(\dot{\gamma})$ must be equal at equal values of frequency and shear rate, can be considered further evidence for a discrimination between polymer solutions and structured systems, at least in first approximation since, as with every rule, it has exceptions.

When oscillatory and steady shear behavior of scleroglucan systems are compared, the traces $\eta^*(\omega)$ and $\eta(\dot{\gamma})$ are almost parallel, with $\eta^*(\omega)$ sensibly higher than $\eta(\dot{\gamma})$, as clearly exemplified in Fig. 12 for the scleroglucan system with $C_p = 2.00$, thus confirming the failure of the Cox–Merz rule. This observation suggests that different types of molecular rearrangements are occurring in both flow patterns, over the frequency and shear rate range considered; in other words, for these systems there is evidence for a short range interaction mechanism, involving time- and strain-dependent intermolecular interactions over and above entanglement coupling, which may influence the small deformation measurements but be effectively destroyed in steady shear flow. These features are again consistent with the presence of a tenuous, transient network, involving non-covalent

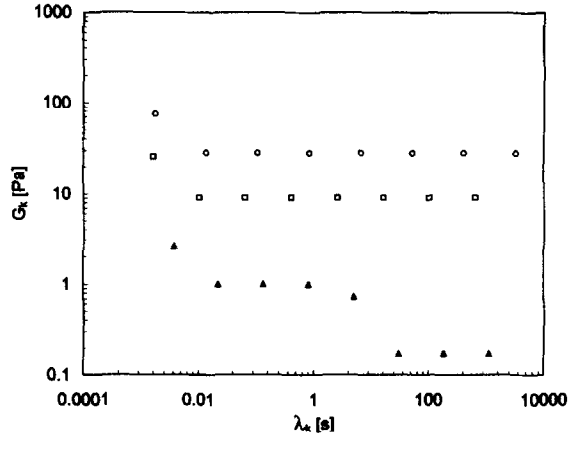

Fig. 11. Relaxation time distribution for the scleroglucan systems reported in Fig. 10: (Δ), $C_p = 0.20$; (□), $C_p = 1.00$; (○), $C_p = 2.00$.

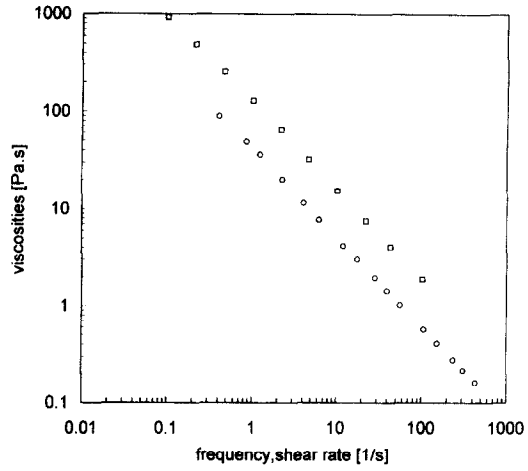

Fig. 12. Combined plot of complex dynamic viscosity $\eta^*(\omega)$ (□) and steady shear viscosity $\eta(\dot{\gamma})$ (○) against frequency, shear rate (Cox–Merz plot) for the scleroglucan system with $C_p = 2.00$. $T = 25°C$.

intermolecular associations, typical of physical weak gel systems.

Non-linear viscoelastic properties

In the case of polymer solutions or weak gels, we can easily extend dynamic measurements to large deformations, or superimposed steady shear flow parallel to oscillatory shear conditions without rupture of the gel or formation of macroscopic discontinuities inside the sample. Physical weak gel systems display non-linear effects, which are similar to those exhibited by many polymer solutions and melts at higher strain amplitudes or by disperse systems, even at low strains. Large-amplitude oscillatory shear is characterized by a stress wave given by equation (3); distortion of the shear stress vs shear strain loops (the so-called Lissajous figures) from an elliptical shape are due to higher harmonics, and the two-fold symmetry of the loops is ensured by the odd value series in equation (3). As the strain amplitude is increased at a given oscillation frequency, the amplitudes of the higher harmonics increase, and so does the distortion (see Fig. 13). Figure 14 shows how the contribution of the third harmonic, expressed as percentage of the fundamental harmonic 100 τ_3/τ_1, increases with increasing strain for the scleroglucan sample with $C_p = 1.13$. At a given strain amplitude, the opposite effect is observed with increasing frequency.

For weak gels as well as for polymer solutions, a strain amplitude increase in the non-linear viscoelastic region produces only a progressive variation, which is slightly dependent on the imposed frequency of oscillation, so that the typical profiles of the viscoelastic quantities are practically maintained. As can be seen in Fig. 15, which refers to a system with $C_p = 1.00$ as an example, an increase in γ^0 beyond the linear viscoelastic regime yields a vertical shifting of G^*, thus indicating a

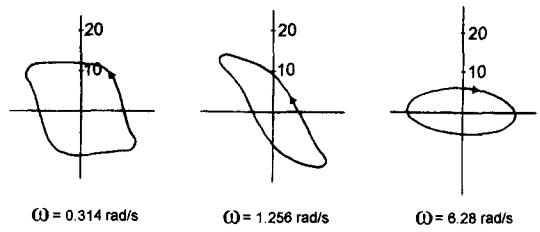

Fig. 13. Lissajous figures in the stress–strain plane for the scleroglucan system with $C_p = 1.00$ at $\gamma^0 = 2.4$ and three different frequencies. $T = 25°C$.

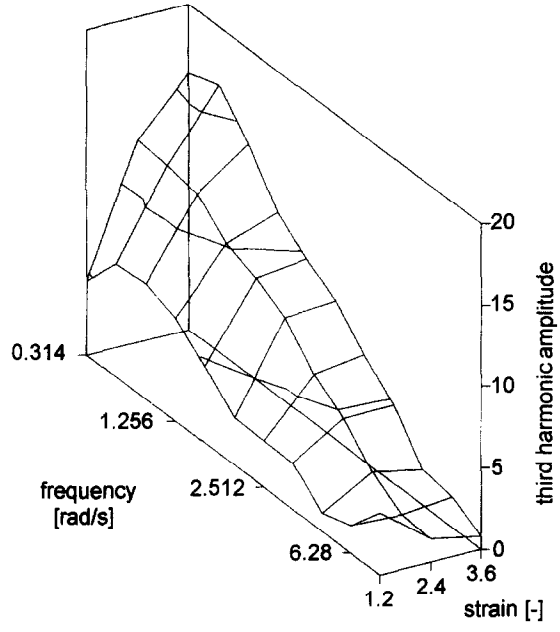

Fig. 14. Third harmonic contribution (expressed as percentage of the fundamental harmonic) as a function of frequency and strain for the scleroglucan system with $C_p = 1.13$. $T = 25°C$.

substantial and predominant decrease of the elastic component.

Let us finally examine the effect of parallel superposition of steady and oscillatory shear flow on the dynamic properties of scleroglucan weak gels, as expressed in the dependence of G^* and δ on the frequency ω. Contrary to what is observed for polysaccharide solutions (Lapasin *et al.*, 1992), a sharp transition in the dependence of G^* and δ on ω is observed with increasing superimposed steady shear rate $\dot{\gamma}$, as we can see for the scleroglucan system with $C_p = 1.00$ reported in Fig. 16a and b. The superimposed steady flow results in a dramatic change of the viscoelastic properties in the medium–low frequency range; in particular, when $\dot{\gamma}$ exceeds a critical value, the profile of the $G^*-\omega$ curve undergoes a strong modification with a low frequency plateau which becomes shear rate-dependent. The low frequency branch of the curve still indicates the persistence of a very weak structure, resulting from the breakdown of the original gel network.

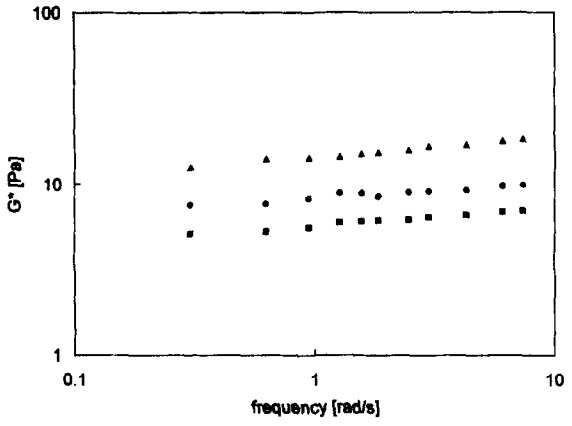

Fig. 15. Complex modulus G^* vs frequency of oscillation ω for the scleroglucan system with $C_p = 1.00$ at three different strains: (▲), $\gamma^0 = 1.2$; (●), $\gamma^0 = 2.4$; (■), $\gamma^0 = 3.6$. $T = 25°C$.

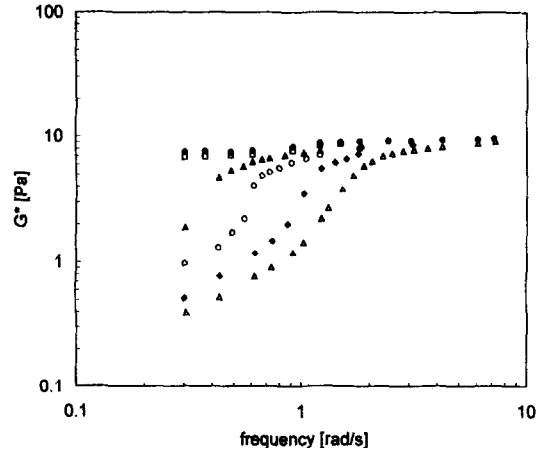

(a)

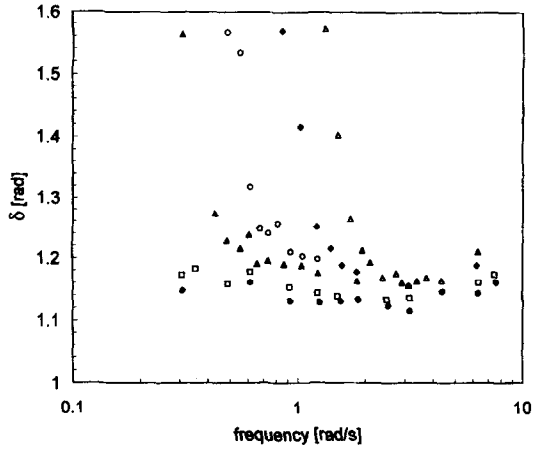

(b)

Fig. 16. (a) Complex modulus G^* and (b) phase lag δ against oscillation frequency for the scleroglucan system with $C_p = 1.00$ at different superimposed parallel rates of shear: (●), $\dot{\gamma} = 0\ s^{-1}$; (□), $\dot{\gamma} = 0.3\ s^{-1}$; (▲), $\dot{\gamma} = 0.6\ s^{-1}$; (○), $\dot{\gamma} = 0.9\ s^{-1}$; (◆), $\dot{\gamma} = 1.5\ s^{-1}$; (Δ), $\dot{\gamma} = 3\ s^{-1}$.

CONCLUSIONS

The rheological behavior of scleroglucan systems both in the sol and gel domain can be described by means of a unique rheological model, resulting from a modification of the original Cross equation, consisting of the introduction of a yield term τ_y. The analysis of the functional behavior of the function $\tau_y(C_p)$ in terms of the percolation theory allowed the determination of the threshold concentration value C_0 for the sol–gel transition which, for the systems considered, corresponds to 0.23. The insensibility to temperature of the rheological behavior of these biopolymer samples has been verified and discussed in terms of two possible mechanisms.

The thixotropic properties of the scleroglucan systems belonging to the weak gel domain have been modeled with a suitable equation and analyzed in terms of the kinetics of both the structural breakdown and build-up processes. Specifically, the structure rehealing processes have been investigated and correlated with a stretched exponential model; the relevant results have shown that a delay time of approximately 4–5 min is necessary to substantially remove shear history and reconfigure the unperturbed state.

The high sensitivity of scleroglucan weak gel systems to strain has been highlighted by means of oscillatory flow tests, performed both in the linear and non-linear viscoelastic regime. In particular, strain sweeps performed at constant frequency of oscillation allowed the determination of the critical strain value.

The shear- and time-dependent behavior, as well as the viscoelastic properties of scleroglucan aqueous systems resulting from our study revealed the existence of a threshold polymer concentration value, above which the peculiar features of these systems are consistent with a picture of a tenuous, transient three-dimensional network (a weak gel), presumably involving the association of the scleroglucan triple helices in a sort of physical junction zone, the exact nature of which still remains to be established.

REFERENCES

Bird, R.B., Dai, G.C. & Yarusso, B.J. (1983). The rheology and flow of viscoplastic materials. *Rev. Chem. Eng.*, **1**, 1–70.

Biver, C., Lesec, J., Allain, C., Salomè, L. & Lecourtier, J. (1986). Rheological behavior and low temperature sol–gel transition of scleroglucan solutions. *Polymer Commun.*, **27**, 351–3.

Bluhm, T.L., Deslandes, Y., Marchessault, R.H., Perez, S. & Rinaudo, M. (1982). Solid state and solution conformation of scleroglucan. *Carbohydr. Res.*, **100**, 117–30.

Brigand, G. (1993). Scleroglucan. In *Industrial Gums: Polysaccharides and their Derivatives*, 3rd edition, eds R.L. Whistler & J.N. BeMiller. Academic Press, New York, pp. 461–74.

Carnali, J.O. (1992). Gelation in physically associating biopolymer systems. *Rheol. Acta*, **31**, 399–412.

Carreau, P.J. (1968). Ph.D. Thesis. University of Wisconsin, Madison, WI, USA.
Cox, W.P. & Merz, E.H. (1958). Correlation of dynamic and steady flow viscosities. *J. Polym. Sci.*, **28**, 619–22.
Cross, M.M. (1965). Rheology of non-Newtonian fluids: a new flow equation for pseudoplastic systems. *J. Colloid Sci.*, **20**, 417–37.
de Gennes, P.-G. (1979). *Scaling Concepts in Polymer Physics*. Cornell University Press, Ithaca & London.
Delben, F., Lapasin, R. & Pricl, S. (1990). Flow properties of *N*-(carboxymethyl) chitosan aqueous systems in the sol and gel domains. *Int. J. Biol. Macromol.*, **12**, 9–13.
Doublier, J.L. & Choplin, L. (1989). A rheological description of amylose gelation. *Carbohydr. Res.*, **193**, 215–26.
Grassi, M., Lapasin, R., Pricl, S. & Colombo, I. (1995). Non-Fickian release from a scleroglucan gel matrix. *Chem. Eng. Comm.*, in press.
Lapasin, R. & Pricl, S. (1995). *Rheology of Industrial Polysaccharides: Theory and Applications*. Blackie Academic & Professional/Chapman & Hall, Glasgow.
Lapasin, R., Pricl, S. & Esposito, P. (1990). Rheological behavior of scleroglucan aqueous systems in the solution and gel domains. In *Rheology of Food, Pharmaceutical and Biological Materials with General Rheology*, ed. R.E. Carter. Elsevier Applied Science, London & New York, pp. 122–32.
Lapasin, R., Pricl, S. & Tracanelli, P. (1992). Different behavior of concentrated polysaccharide systems in large-amplitude oscillating shear fields. *Rheol. Acta*, **31**, 374–80.
Poslinski, A.J., Ryan, M.E., Gupta, R.K., Seshadri, S.G. & Frechette, F.J. (1988). Rheological behavior of filled polymeric systems. I. Yield stress and shear-thinning effects. *J. Rheol.*, **32**, 703–35.
Richardson, R.K. & Ross-Murphy, S.B. (1987). Non-linear viscoelasticity of polysaccharide solutions. 2: Xanthan polysaccharide solutions. *Int. J. Biol. Macromol.*, **9**, 257–64.
Rodgers, N.E. (1973). Scleroglucan. In *Industrial Gums: Polysaccharides and Their Derivatives*, 2nd edition, eds R.L. Whistler & J.N. BeMiller. Academic Press, New York, pp. 499–511.
Sandford, P.A. (1982). Potentially important microbial gums. In *Food Hydrocolloids*, Vol. 1, ed. M. Glicksman. CRC Press, Boca Raton, pp. 167–202.
Trapeznikov, A.A. & Fedotova, V.A. (1954). Methods for thixotropy evaluation in liquid–plastic colloidal systems. *Dokl. Akad. Nauk. SSSR*, **95**, 595–8.
Yanaki, T., Kojima, T. & Norisuye, T. (1981). Triple helix of scleroglucan in dilute sodium hydroxide. *Polymer J.*, **13**, 1135–42.
Yanaki, T. & Norisuye, T. (1983). Triple helix and random coil of scelorglucan in dilute solutions. *Polymer J.*, **15**, 389–96.
Yang, T.M.T. & Krieger, I.M. (1978). Comparison of methods for calculating shear rates in coaxial viscosimeters. *J. Rheol.*, **22**, 413–21.

APPENDIX

Under continuous shear flow conditions, the viscosity of a weak gel system is determined by the dimensions of the flow units and their variations in shape and size with the imposed flow conditions, in absolute analogy to what is observed for aggregated particle suspensions.

Therefore, the correlation of data obtained from step-wise procedures and the interpretation of both shear- and time-dependent properties can be performed on the bases of a rheological model, resulting from the combination of an equation of state and a rate equation describing the kinetics of the structural processes induced by changes in the imposed shear conditions. As for aggregated particle suspensions, the state equation can be conveniently formulated in terms of relative viscosity η_r and of effective volume fraction Φ_{eff} occupied by the flow units (i.e. the gel fragments) which are present under flow conditions. Φ_{eff} is greater for more extended particle aggregation, and has an upper limit corresponding to the maximum packing condition Φ_m.

For aggregated suspensions, the functional dependence of η_r on Φ_{eff} can be suitably described by the following expression, which can be reasonably used also in the case of weak gels:

$$\eta_r = \left(1 - \frac{\Phi_{eff}}{\Phi_m}\right) \tag{A1}$$

The variation of Φ_{eff} with the shear rate $\dot{\gamma}$ and time t can be derived from the following rate equation:

$$\frac{d\Phi_{eff}}{dt} = K_f(\Phi_{eff,max} - \Phi_{eff}) - K_b(\Phi_{eff} - \Phi_{eff,min}) \tag{A2}$$

where $\Phi_{eff,max}$ and $\Phi_{eff,min}$ represent the maximum and the minimum value of Φ_{eff}, respectively, and Φ_{eff} is the instantaneous value of the effective volume fraction, which depends upon the flow conditions present at time t. K_f and K_b are rate constants, which modulate the kinetics of the structural build-up and breakdown processes, respectively; K_f depends on temperature whereas K_b is a function of the applied shear rate $\dot{\gamma}$.

By considering both the rate equation (A2) and the dependence of K_b on $\dot{\gamma}$, we obtain the expression for the variation of Φ_{eff} with $\dot{\gamma}$ under steady shear conditions:

$$\frac{d\Phi_{eff}}{dt} = 0 \rightarrow \Phi_{eff,s}(\dot{\gamma}) = \frac{\Phi_{eff,max} + \dfrac{K_b}{K_f}\Phi_{eff,min}}{1 + \dfrac{K_b}{K_f}} \tag{A3}$$

From the combination of equations (A1) and (A3) we now obtain the relationship describing the shear-dependent behavior of these systems under steady shear conditions as follows:

$$\tau_s(\dot{\gamma}) = \eta_s \eta_r \dot{\gamma} \tag{A4}$$

Under constant shear rate conditions, K_b is also constant, so that the variation of Φ_{eff} with time t can be derived from the rate equation as:

$$\Phi_{eff}(t) = \Phi_{eff,s} + (\Phi_{eff,i} - \Phi_{eff,s}) \exp(-(K_f + K_b)t) \tag{A5}$$

where $\Phi_{eff,i}$ is the initial value of the effective volume fraction in the $\tau(t)$ transient at a given constant $\dot{\gamma}$.

As a consequence of the development described

above, we obtain the following expression for the stress transients $\tau(t)$ at constant $\dot{\gamma}$:

$$\frac{\frac{1}{\sqrt{\tau}} - \frac{1}{\sqrt{\tau_s}}}{\frac{1}{\sqrt{\tau_i}} - \frac{1}{\sqrt{\tau_s}}} = \exp(-Kt) \tag{A6}$$

in which $K = K_f + K_b$.

The application of the present model to the data sets obtained from the multiple-step procedure on scleroglucan systems allows us only to draw some information on its adaptability to the considered cases. Indeed, the kinetic constant K depends on the instantaneous shear rate only, and cannot be a function of the previous rheological history experienced by the sample. In other words, K must have the same value for both the build-up and the breakdown structural processes which take place at the same shear rate.

From the handling of the relevant experimental data, we have seen that such condition of equal kinetics for the two structural processes is not satisfied. Therefore, for a rigorous application of this model to our experimental data, we should have modified the rate equation (A2) and the following model derivation by considering two different orders for the two structural processes, the order of the breakdown process being, however, higher than that of the corresponding build-up. This modification is not as simple as it might seem, as it involves a very heavy mathematical treatment. Therefore, since the model proposed in the text is simple enough and the relevant results are quite satisfactory, we consider its presentation outside the scope of the present paper.